Elongated Wire-Like Zinc Oxide Nanostructures Synthesized from Metallic Zinc

El-Shazly M. Duraia[1,2*], G.W. Beall[3], Zulkhair A. Mansurov[4], Tatyana A. Shabanova[4], Ahmed E. Hannora[1]

[1]Texas State University-San Marcos, Department of Chemistry and Biochemistry, San Marcos, TX 78666, USA
[2]Suez Canal University, Faculty of Science, Physics Department, Ismailia Egypt.
[3]Distinguished adjunct professor, Faculty of Science, King Abdulaziz University, Jeddah, Saudi Arabia
[4]The Institute of Combustion Problems, Almaty, Kazakhstan

Abstract

Elongated wire-like Zinc oxide, nanocombs and nanocrystals have been successfully synthesized on the silicon substrate from the metallic zinc as a starting material. The annealing temperature was as low as 450 ºC in argon atmosphere mixed with about 3% oxygen. Structural analysis using the X-ray Diffraction (XRD) and Transmission Electron Microscopy (TEM) showed that the existence of two phases; nanowires and crystalline form. Moreover some nanoparticles aggregates were noticed to be attached in the bulk to the sides of the ZnO nanocrystals and sometimes these aggregate attached to the Zinc oxide hexagonal crystal and grow to form nanowire at different angles. Scanning electron microscopy (SEM) investigations for the zinc oxide nanostructure on the silicon substrate showed the formation of the nanocrystals in the gas flow direction and at the low energy sites over the silicon substrate. Photoluminescence (PL) measurements, performed at the room temperature, showed the existence of two basic emissions: narrow ultraviolet (UV) emission at 398 nm which attributed to the near band edge emission of the wide band gap and a very wide, more intensive, green emission at 471 nm corresponds to the crystal defects such as vacancies, interstitial sites in ZnO.

Introduction

The last two decades witnessed an intensive work on the one dimensional nanostructures such as nanotubes and nanowires [1-5]. Among these nanostructures Zinc oxide (ZnO) has attracted the scientific community due to its exceptional structural and physical properties and the promising applications especially in optoelectronics. ZnO is a semiconductor with large band gap and exciton binding energy that could lead to lasing action based on exciton recombination and possibly polariton and exciton interaction even above room temperature. ZnO has many versatile applications for in light-emitting diodes, optoelectronic devices, sensors and catalysts [6, 7]. Recently the potential of converting mechanical energy to electrical energy has been report utilizing the piezoelectric effect observed in ZnO nanowires [8].

Generally, ZnO nanostructures can be synthesized by sol-gel technique [9], hydrothermal synthesis [10], thermal oxidation [11], and chemical vapor deposition (CVD) [12]. Hydrothermal synthesis is known as a simple and cheap method for the nanostructures synthesis; however the hydrothermal crystals inevitably incorporate alkali metals and small amounts of metallic impurities from the solution. Among all growth methods, CVD technology is particularly interesting not only because it gives rise to high-quality films but also because it is applicable to large-scale production. ZnO deposition occurs as a result of chemical reactions of vapor-phase precursors on the substrate, which are delivered into growth zone by the carrier gas. The reactions take place in a reactor where a necessary temperature profile is created in the gas flow direction.

Herein; zinc oxide nanostructures with different morphologies have been synthesized on silicon substrate using metallic zinc as a starting material. Elongated wire-like Zinc oxide, nanocombs and nanocrystals have been successfully synthesized.

* Corresponding author. E-mail: duraia_physics@yahoo.com

The annealing temperature was as low as 450 °C in argon atmosphere mixed with about 3% oxygen. The as-synthesized products have been characterized by SEM, TEM and XRD and the PL spectrum has been discussed.

Zinc Oxide Nanostructures Preparation

Metallic Zinc was used as a starting material to produce the zinc oxide nanostructures. The metallic zinc was placed at the middle part of the tube furnace as used in [4]. Silicon wafer substrate was placed at a distance of 1 cm from the metallic zinc in the Ar (with about 3% oxygen) flow direction. The gas flow rate was 2 L/min. the furnace was heated to 450 °C and the samples were annealed for 30 min. after that the furnace was naturally cooled to the room temperature after that large quantity of a white fiber material was formed inside the furnace around and over the silicon substrate. This white fiber was noticed to be not well attached to the substrate has been analyzed.

The samples were studied using the scanning electron microscope JEOL JSM-6490LA with resolution (3 nm), and energy dispersed X-ray spectroscopy which is being attached to the SEM, Transmission electron microscope JEM 100CX accelerating voltage 100 kV. The photoluminescence (PL) measurements were carried out at the room temperature. The PL excitation was performed by 325 nm-He–Cd laser. The film structures were investigated by X-ray diffraction using photographic registration of X-ray reflections. The X-ray diffraction patterns were obtained with the help of collimated (0.05 × 1.5 mm^2) monochromatic (Cu Kα) beam directed at an angle of 5° to sample surface.

Results and Discussion

Structure and Morphological Analysis

X-ray diffraction (XRD) was performed to analyze the crystallinity of the precursors and produced zinc oxide nanostructures. Figure 1 represents the XRD pattern of the raw zinc and the zinc oxide nanowires. The diffraction peaks are very sharp and quite intense. In the first curve the XRD pattern matches the standard JCPDS data (card no. 04-0831) of Zn. The space group is P63/mnc with a = 2.665 Å, c = 4.947 Å and c/a = 1.8563. The unit cell of the crystal is hexagonal with the presence of the peaks (0 0 2), (1 0 0), (1 0 1) and (1 0 2). For the second curve, it can be seen that all the reflection peaks of the products can be readily indexed to pure ZnO with wurtzite structure (JCPDS36-1451). The broad peak centered at 2θ = 21 indicates that there is an amorphous phase. No impurities could be observed in these patterns which also confirmed from the EDAX analysis that showed only zinc and oxygen elements.

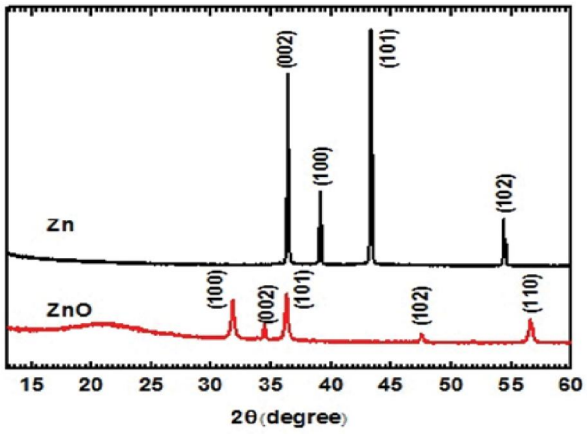

Fig. 1. XRD of the ZnO nanowires.

The TEM investigations showed that there are several phases. The presence of the rings and the dots in the microdiffraction pattern indicates the presence of at least two phases. There are elongated nanostructures of two types: nanowires (Fig. 2c) with 20-30 nm in diameter and length ranges from 0.5 μm to several micrometers and a more traditional bulk crystalline form (Fig. 2d). The products were not a pure crystalline but also contain amorphous phase. The same result was also noticed from the XRD. Elongated crystallites form aggregates, which remained stable at the corners of the crystals. Sometimes the growths in bulk volume along one side of the crystal (Fig. 2 e), and sometimes splice sites are included and the ZnO aggregates on the faces of the hexagonal crystal and grow to form nanowires at different angles from the same crystal. As one can see from Fig. 2f, nanowires grow on the faces of a pure hexagonal zinc oxide crystal. The size of the hexagonal crystal is 40 nm and the grown nanowires about 300 nm in length while its diameter is very close to the crystal size. Elongated particles formed in the wire-like elongated structure (Fig. 2a); in the literature there are no reports about such morphology for the zinc oxide.

Figure 3 depicts the SEM images of the as-synthesized ZnO nanostructures. As clearly seen from the figure, the ZnO uniformly cover all the substrate and grows on the low energy sites of the silicon substrate and on the gas flow direction. There are many forms of the ZnO nanostructures on the same sample in crystalline form and in the wire-like elongated form. Some nanocombs were found to be formed perpendicular to the substrate with 2 μm in height and few micrometers in length.

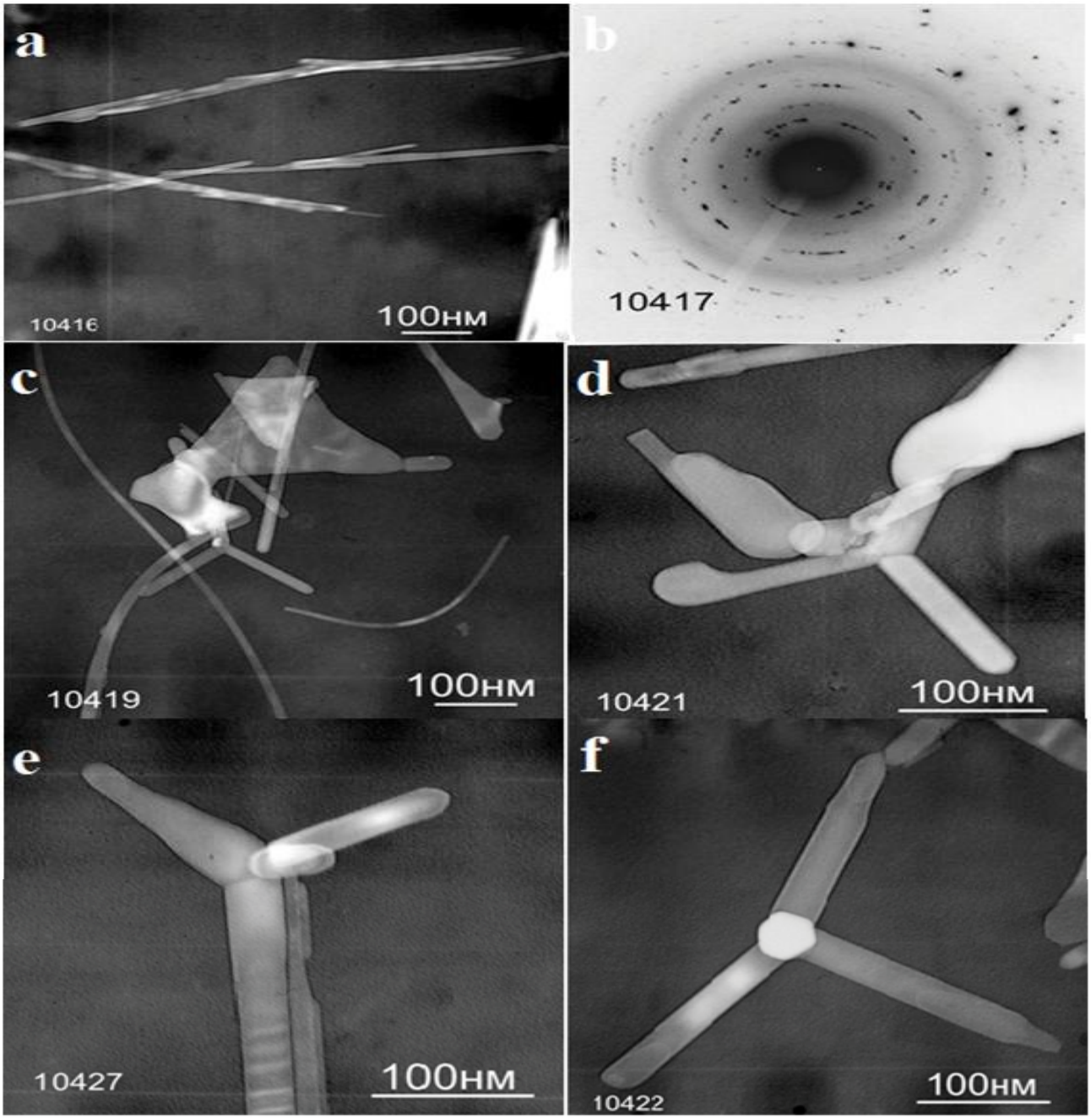

Fig. 2. TEM of the ZnO nanostructures and the microdiffraction.

Ren et al. have used the metallic zinc blocks to grow catalyst free zinc oxide nanowires array on zinc substrate below the melting point in air [11]. In our work, no zinc oxide nanostructures have been observed below the temperatures 450 ºC. Depending on the available information it is hard to explain the growth of these nanostructures without catalyst. Ren suggested the diffusion of either the metal atom or oxygen atoms through the oxide layer which formed over the metallic zinc substrate. The situation is different in our case since the zinc nanostructures have been grown directly over the silicon substrate as well as the higher temperature have been used in our case is higher than the zinc melting point. The amount of zinc oxide nanostructure is noticeably increased when the temperature increased to 550 ºC and the annealing time increased to one hour. As one can see from Fig. 4a most of the product is two dimensional nanostructures their length might go to several tens of micrometers. Moreover in Fig. 4c some crystals with nanorods at their end. The diameter of these nanorods was 30-40 nm. It

is interesting to notice that regardless of the size of the crystals, these nanorods have the same diameter. Small amount of zinc oxide nanostructure of similar morphology have been noticed also at the lower annealing temperature as shown in Fig. 5. As shown in the figure star-like ZnO nanostructures which grown in all directions have been observed; sometimes it consists of central axis from which the hexagonal sheet-like ZnO can grow with very sharp end. Zinc oxide nanostructures with similar morphology have been reported by Tang et al.; the authors concluded that the first step is the formation of ZnO film on the substrate. Then anisotropic abnormal grain growth in the form of ZnO platelets takes place. Subsequently, single-crystalline ZnO platelets grow in [0001] direction to form whiskers [13].

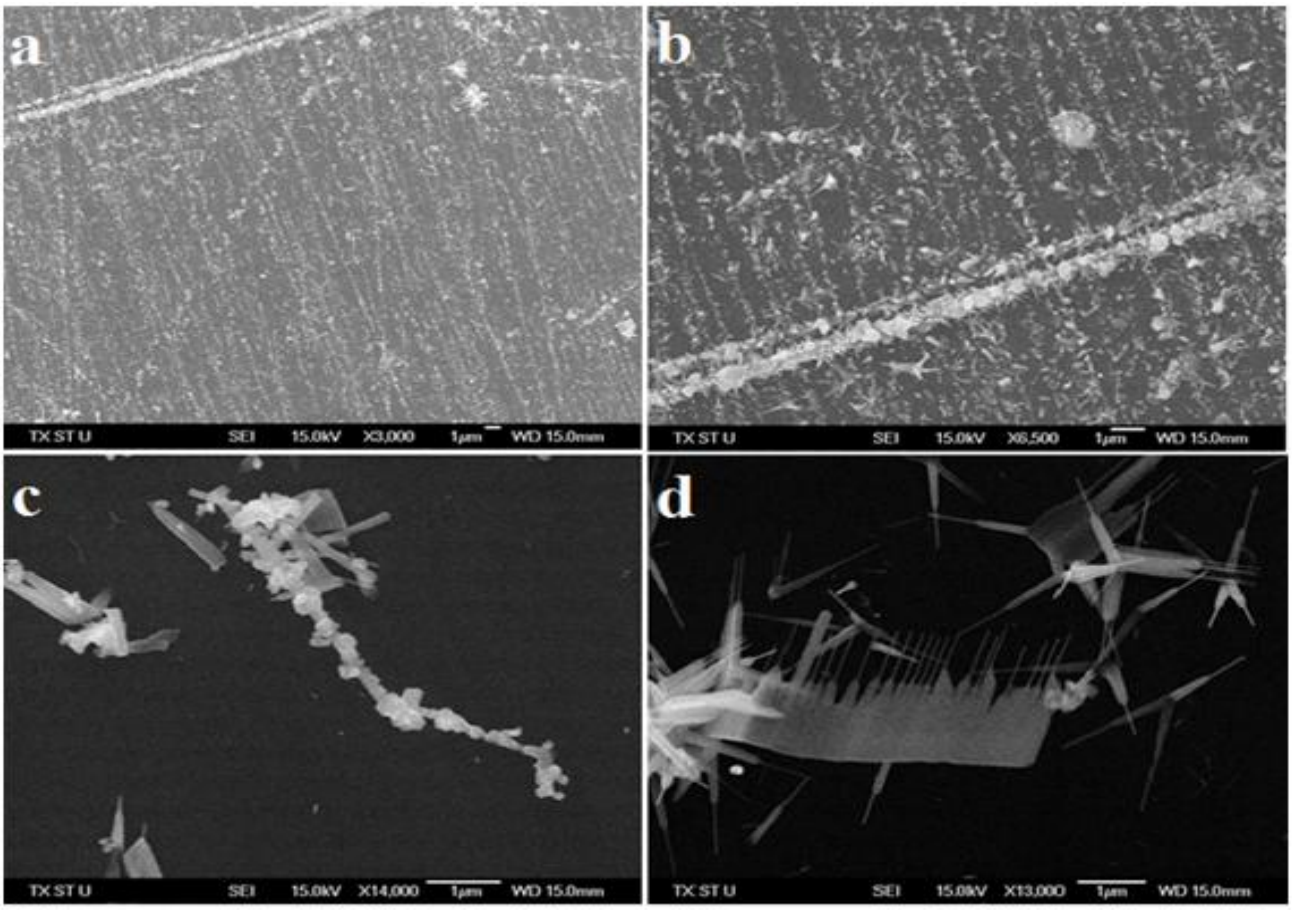

Fig. 3. The SEM images of the as-synthesized ZnO nanostructures on silicon substrate.

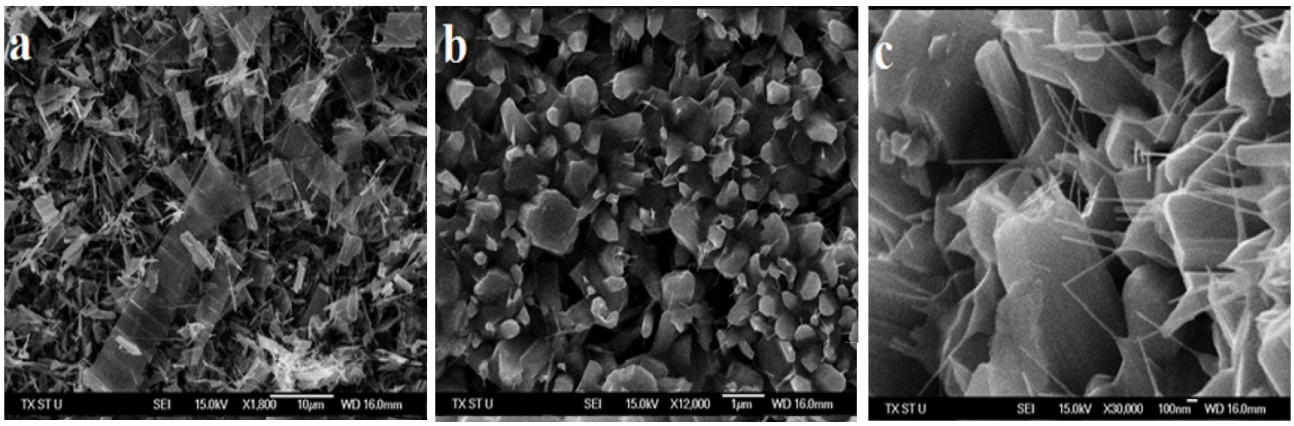

Fig. 4. SEM images of the ZnO nanostructures grown at 550 ºC for one hour.

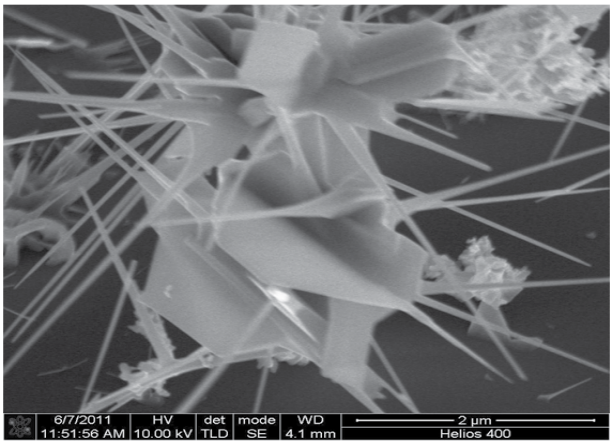

Fig. 5. Star-like ZnO nanostructure.

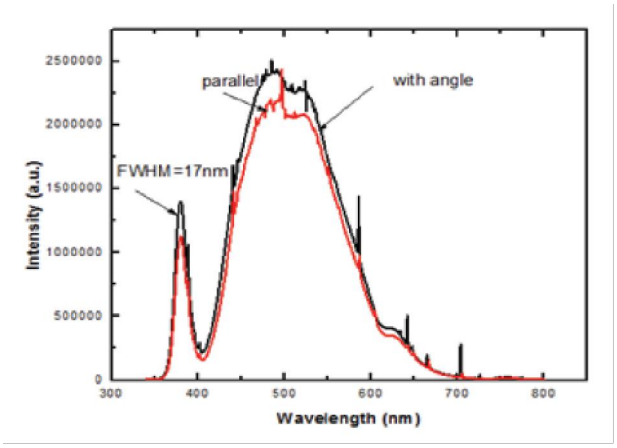

Fig. 6. The typical PL spectrum of the as-synthesized ZnO nanostructures.

PL

PL measurements are performed in order to investigate optical properties of the ZnO nanostructures. All the PL measurements were performed at the room temperature using the He–Cd laser with the 325 nm excitation wavelength. The typical PL spectrum of the as-synthesized ZnO nanostructures is represented in Fig. 6. As seen from the figure there are two basic peaks, the narrow ultraviolet (UV) emission at 398 nm (Full width at half maximum FWHM = 17 nm) and a very wide green emission at 471 nm which is relatively more intensive than the UV one. Authors in ref. [11] have reported a similar PL spectrum which has only the UV- emission. The PL measurements were done when the sample is parallel to the laser beam and when it makes an angle 30 with the laser beam. It was noticed that the intensity of the spectrum decreased when the sample was parallel to the laser and this decrease in the intensity could be attributed to the polarization effect. It was quite interesting to observe that both the green and UV- bands in the PL spectrum of the zinc oxide possess the polarization effect; this also has been reported by the other authors [14]. Figure 7 represents the PL of the ZnO nanostructures on the silicon substrate and the fiber collected from the furnace and around the silicon. As one can see from the figure the wide green peak has completely disappeared in the case of the white fiber where the UV peak was more intensive with higher FWHM than the green one. Moreover; from the magnified graph in the infra-red part, one can notice the existence of the small peak for both types of the ZnO. This IR peak was found at 757 nm for the ZnO on silicon while this peak located at 761 nm for the white fiber also the intensity for the intensity is much higher in the white fiber case, as indicated in the magnified graph in Fig. 7.

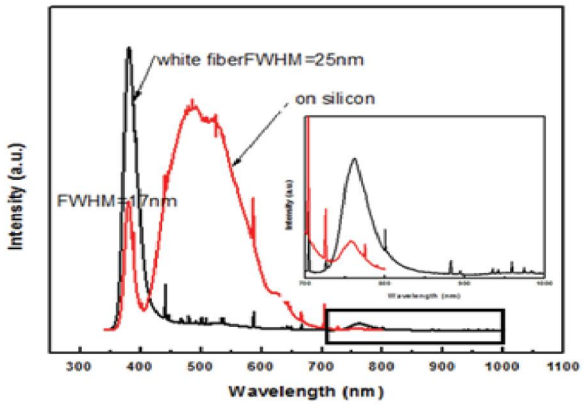

Fig. 7. The PL of the ZnO nanostructures on the silicon substrate and the fiber collected from the furnace and around the silicon.

It is well known that, the UV emission was attributed to the near band edge emission of the wide band gap ZnO, which is responsible for the excitonic recombination. It has been already demonstrated that, the green band emission corresponds to the crystal defects such as vacancies, interstitial sites in ZnO. These green emissions originated from the recombination of the holes with the electrons occupying the singly ionized oxygen vacancies [15]. The mechanism of the green emission has been suggested to be mainly due to the concentration of free electrons and the existence of various point defects due to heating treatments or oxidation associated with our process that could have easily formed the recombination centers [16]. Umar et al. reported that the intensity of the UV emission was related to the crystal quality of the deposited materials and therefore a good crystal quality (fewer structural defects and impurities, etc.) may enhance the intensity of the UV emission as compared to the green emission [17].

Conclusion

For the first time, Elongated wire-like Zinc oxide and zinc oxide nanostructures with different morphologies have been synthesized on silicon substrate using metallic zinc as a starting material without using any catalyst. The annealing temperature was as low as 450 ºC in argon atmosphere mixed by about 3% oxygen. XRD and EDAX analysis showed that the material product is pure and contains zinc and oxygen only. TEM investigations showed the presence of two phases' nanowires and crystalline form. Room temperature PL measurements showed two basic peaks, the narrow UV emission at 398 nm and a very wide green emission at 471 nm which is relatively more intensive than the UV one. The simplicity and low cost of this method opens the door for the growth of pure zinc oxide nanostructure directly from the metallic zinc for the different applications.

References

1. C. Rao, A. Govindaraj, G. Gundiah, S. Vivekchand. Nanotubes and nanowires. Chemical Engineering Science, 59 (2004) 4665-4671.
2. E-S.M. Duraia, Zulkhair Mansurov, S. Zh. Tokmoldin. Preparation of carbon nanotubes with different morphology by microwave plasma enhanced chemical vapour deposition. Physica status solidi (c), 7 (2010) 1222-1226.
3. E-S.M. Duraia, Kh.A. Abdullin. Ferromagnetic resonance of cobalt nanoparticles used as a catalyst for the carbon nanotubes synthesis. Journal of Magnetism and Magnetic Materials, 321(2009) L69-L72.
4. E-S.M. Duraia, Z.A. Mansurov, S. Tokmoldin, Gary W. Beall. Preparation of highly aligned silicon oxide nanowires with stable intensive photoluminescence. Physica B: Condensed Matter, 405 (2010) 1176-1180.
5. E-S. M. Duraia, Z.A. Mansurov, S. Tokmoldin. Synthesis, characterization and photoluminescence of tin oxide nanoribbons and nanowires. Physica B: Condensed Matter, 404 (2009) 3952-3956 .
6. X.L. Hu, Y.J. Zhu, S.W. Wang. Sonochemical and microwave-assisted synthesis of linked single-crystalline ZnO rods. Mater. Chem. Phys. 88 (2004) 421.
7. R. Wahab, S.G. Ansari, Y.S. Kim, H.K. Seo, G.S. Kim, G. Khang, H.S. Shin. Mater. Res. Bull. 42 (2007) 1640.
8. Z. Lin Wang, J. Song. Piezoelectric nanogenerators based on zinc oxide arrays. Science, 312 (2006) 242-246.
9. M. Çopuroğlu, S.O' Brien, Gabriel M. Crean. Sol-gel synthesis, comparative characterisation, and reliability analyses of undoped and Al-doped zincoxide thin films. Thin Solid Films 517 (2009) 6323-6326.
10. J. Joo, B. Chow, M. Prakash, E. Boyden & J. Jacobson. Face-selective electrostatic control of hydrothermal zinc oxide nanowire synthesis. Nature Materials 10 (2011) 596-601.
11. S. Ren, Y.F. Bai, Jun Chen, S.Z. Deng, N.S. Xu, Q.B. Wu, Shihe Yang. Catalyst-free synthesis of ZnO nanowire arrays on zinc substrate by low temperature thermal oxidation. Materials Letters 61 (2007) 666-670.
12. B. Xiang, P. Wang, X. Zhang, S. Dayeh, D. Aplin, C. Soci, D. Yu, D. Wang. Rational Synthesis of p-Type Zinc Oxide Nanowire Arrays Using Simple Chemical Vapor Deposition. Nano Lett., 7 (2007).
13. H. Tang, J. Chang, Y. Shan, D. Ma, Tsz-Yan Lui et al. Growth mechanism of ZnO nanowires via direct Zn evaporation. J. Mater. Sci. (2009) 44:563-571.
14. N.E. Hsu, W.K. Hung, and Y.F. Chen. Origin of defect emission identified by polarized luminescence from aligned ZnO nanorods. J. Appl. Phys., Vol. 96, No. 8, 15 October 2004.
15. K. Vanheusden, W.L. Warren, C.H. Seager, D.R. Tallant, J.A. Voigt, B.E. Gnade. Mechanisms behind green photoluminescence in ZnO phosphor powders. J. Appl. Phys. 79 (1996) 7983-7990.
16. R. Dingle. Luminescent transition associated with divalent copper impurities and green emission from semiconducting zinc oxide. Phys. Rev. Lett. 23 (1969) 579-581.
17. A. Umar, Y.B. Hahn. ZnO nanosheet networks and hexagonal nanodiscs grown on silicon substrate: growth mechanism and structural and optical properties. Nanotechnology 17 (2006) 2174-2180.

Received 24 August 2012